Visualizing the extra symmetry of the Kepler problem

Jim Morehead

Citation: American Journal of Physics **73**, 234 (2005); doi: 10.1119/1.1791272
View online: https://doi.org/10.1119/1.1791272
View Table of Contents: https://aapt.scitation.org/toc/ajp/73/3
Published by the American Association of Physics Teachers

Visualizing the extra symmetry of the Kepler problem

Jim Morehead[a)]
120 Holly Court, Mountain View, California 94043

(Received 9 March 2004; accepted 16 July 2004)

The extra symmetry of the Kepler problem corresponding to the conservation of the Runge–Lenz vector can be visualized by studying how entire Kepler ellipses evolve under symmetry transformations. After discussing the general case, we show that the evolution generated by a component of the Runge–Lenz vector in the plane of the orbit yields the same family of ellipses in the plane as the projection onto the plane of a rotation of a certain circle in three dimensions.
[DOI: 10.1119/1.1791272]

I. INTRODUCTION

The classical two-body $1/r^2$ force problem has many special properties. The best known is that all of its bound orbits are closed. The reason is that there is an extra quantity, the Runge–Lenz vector, conserved by the motion in addition to the angular momentum, which is conserved by all central forces. This extra conserved vector has a clear physical interpretation: it points in the direction of the perihelion (closest approach) and its magnitude is proportional to the eccentricity of the ellipse. The fact that the vector does not change along the orbit can be interpreted as there being no precession or change in shape: a closed orbit (see, for example, Ref. 1).

Equivalently, the problem has extra symmetry in addition to the rotational symmetry common to all central forces. The whole symmetry group is $O(4)$, all orthogonal transformations (rotations) on four-dimensional space. This generalization from the symmetry group $O(3)$ of rotations of physical space is somewhat abstract. The fictitious fourth dimension does not behave in a straightforward way. For example, a physical rotation has a simple action on phase space: the position and momentum are separately and identically rotated. In the extra symmetry the position and momentum are coupled and the symmetry trajectories generated in phase space are complicated.

How can we obtain a physical intuition for the extra symmetry, as we have for the extra conservation law? In this paper we suggest that the extra symmetry is easy to visualize in terms of its action on entire orbits instead of on individual points in phase space. The flow generated by a given component of the Runge–Lenz vector takes a given Kepler ellipse (given values of the major axis, eccentricity, and orientation) through other ellipses of different eccentricities and possibly different orientations, but with the same length of the major axis. This length is preserved as well as the energy because the energy of an ellipse depends on only the length of the major axis and not on the eccentricity or orientation. The extra symmetry is, in a sense, the independence of the energy on the eccentricity.

We derive the family generated by any component of the Runge–Lenz vector acting on any Kepler ellipse. Although the general family is not difficult to characterize, the special cases of the symmetry generated by the component of the Runge–Lenz vector perpendicular to the plane of the orbit and by a component of the Runge–Lenz vector in the plane of the orbit are particularly easy to visualize. For example, the evolution generated by a component of the Runge–Lenz vector in the plane of the orbit keeps the orbit in the plane. The sequence of ellipses traced out in the plane is (when drawn centered at the origin) the same as the projection onto the plane of the rotation of a certain circle in three dimensions.

II. CONSERVATION AND SYMMETRY

In addition to conserving angular momentum $\mathbf{L}=\mathbf{r}\times\mathbf{p}$, the Kepler problem, with the Hamiltonian

$$H(\mathbf{r},\mathbf{p})=\frac{1}{2m}(p_x^2+p_y^2+p_z^2)-\frac{k}{r}, \tag{1}$$

also conserves the Runge–Lenz vector,

$$\mathbf{M}=\frac{1}{m}\mathbf{p}\times\mathbf{L}-k\frac{\mathbf{r}}{r}, \tag{2}$$

where $k=Gm_1m_2$ and m is the reduced mass, $m_1m_2/(m_1+m_2)$. The closing of the orbits can be understood by this extra conservation. The motion under a general central force conserves the Hamiltonian and the angular momentum vector, a total of four functions. The trajectory must lie on the level set of these four functions in six-dimensional phase space, which is a two-dimensional surface, corresponding to planar central-force orbits. The Kepler Hamiltonian conserves these four plus the three components of the Runge–Lenz vector. Not all seven functions are independent. Two constraints follow from the facts that

$$\mathbf{L}\cdot\mathbf{M}=0, \quad |\mathbf{M}|^2=k^2\left(1+\frac{2HL^2}{mk^2}\right). \tag{3}$$

Equation (3) leaves five independent constraints in six dimensions, leaving a one-dimensional space for the trajectory—a closed orbit.

In classical mechanics there is a one-to-one correspondence between conservation laws and symmetry. A function that is a constant of the motion serves as the generator of a symmetry of the system. This connection is most easily studied in the Hamiltonian formulation. There the rate of change of a function in phase space $A(\mathbf{r},\mathbf{p})$ along a trajectory of the Hamiltonian $H(\mathbf{r},\mathbf{p})$ can be written as

$$\frac{dA}{dt}=\frac{\partial A}{\partial x_i}\frac{dx_i}{dt}+\frac{\partial A}{\partial p_i}\frac{dp_i}{dt}=\frac{\partial A}{\partial x_i}\frac{\partial H}{\partial p_i}-\frac{\partial A}{\partial p_i}\frac{\partial H}{\partial x_i}=\{A,H\}, \tag{4}$$

where the sum over i from 1 to 3 is implicit. The bracket on the right is the Poisson bracket.

If the function A is conserved along the trajectories of H, then

$$\frac{dA}{dt}=\{A,H\}=0, \tag{5}$$

that is, A and H commute. Conversely, the value of H is conserved under the motion generated by A. That is, the value of H does not change along a trajectory generated by A,

$$\frac{dH}{d\lambda}=\{H,A\}=0, \tag{6}$$

where λ is used instead of t to remind us that the evolution parameter is not a physical time. Equation (6) implies that H is invariant under the symmetry transformation generated by A.

A standard example is angular momentum. For any constant unit vector $\hat{\mathbf{n}}$, the function $A=\hat{\mathbf{n}}\cdot\mathbf{L}$ generates the motion

$$\frac{d\mathbf{r}}{d\lambda}=\frac{\partial A}{\partial \mathbf{p}}=\hat{\mathbf{n}}\times\mathbf{r}, \tag{7a}$$

$$\frac{d\mathbf{p}}{d\lambda}=-\frac{\partial A}{\partial \mathbf{r}}=\hat{\mathbf{n}}\times\mathbf{p}, \tag{7b}$$

which is a rotation about the axis $\hat{\mathbf{n}}$. Equation (7) implies that the symmetry of a system under rotations about the axis $\hat{\mathbf{n}}$ is equivalent to the conservation of the component of angular momentum in the direction $\hat{\mathbf{n}}$.

The components of the Runge–Lenz vector generate trajectories that are much more complicated. Hamilton's equations for the general component $\hat{\mathbf{n}}\cdot\mathbf{M}$ are

$$\frac{d\mathbf{r}}{d\lambda}=\frac{1}{m}[\mathbf{r}\times(\mathbf{p}\times\hat{\mathbf{n}})-\hat{\mathbf{n}}\times(\mathbf{r}\times\mathbf{p})], \tag{8a}$$

$$\frac{d\mathbf{p}}{d\lambda}=-\frac{1}{m}\mathbf{p}\times(\hat{\mathbf{n}}\times\mathbf{p})+\frac{k}{r^3}\mathbf{r}\times(\hat{\mathbf{n}}\times\mathbf{r}). \tag{8b}$$

The position and momentum variables are coupled, implying that the symmetry cannot be thought of as acting on real space, but rather on all of phase space. The trajectories cannot be expressed in closed form and are not closed.

The Poisson brackets of all the generators with each other helps to elucidate the symmetry group. Simple calculations reveal that

$$\{L_i,L_j\}=\epsilon_{ijk}L_k, \tag{9a}$$

$$\{M_i,L_j\}=\epsilon_{ijk}M_k, \tag{9b}$$

$$\{M_i,M_j\}=(-2H(\mathbf{r},\mathbf{p})/m)\epsilon_{ijk}L_k. \tag{9c}$$

Equation (9b) says that $\mathbf{M}(\mathbf{r},\mathbf{p})$ is a vector function (that is, it rotates properly). Equation (9c) hints that we should rescale the Runge–Lenz vector as

$$\mathbf{M}^*(\mathbf{r},\mathbf{p})=\mathbf{M}(\mathbf{r},\mathbf{p})/\sqrt{-2H(\mathbf{r},\mathbf{p})/m} \tag{10}$$

on the part of phase space where the energy is negative (bound orbits). Because the Hamiltonian commutes with all the symmetry generators, the commutation relations of the rescaled Runge–Lenz vector are simply

$$\{L_i,L_j\}=\epsilon_{ijk}L_k, \tag{11a}$$

$$\{M_i^*,L_j\}=\epsilon_{ijk}M_k^*, \tag{11b}$$

$$\{M_i^*,M_j^*\}=\epsilon_{ijk}L_k. \tag{11c}$$

If we consider a fictitious fourth dimension and define $M_k^*=x_4p_k-x_kp_4$, then the relations (11) are the angular momentum commutation of rotations in four dimensions.[2]

The symmetry trajectories generated by a component $\hat{\mathbf{n}}\cdot\mathbf{M}^*$ are closed (see the end of Sec. V), unlike those of the original vector $\mathbf{M}$. However the trajectories cannot apparently be written down in closed form and are probably not a great help for developing intuition.

III. ACTIONS ON ORBITS

It is much easier to understand the flow generated by a component M_k^* by studying how an entire Kepler ellipse evolves: take all points in phase space on a given Kepler ellipse and flow each under M_k^* for a ''time'' λ. The Poisson commutativity of H and M_k^* implies that the flows of those two functions commute. That is, flow under H for t then flow under M_k^* for λ is the same as flow under M_k^* for λ then flow under H for t. This equivalence implies that an initial Kepler ellipse flows under M_k^* into another Kepler ellipse of the same energy.

The evolution of the ellipses is easy to study because an ellipse is completely specified by its values of $\mathbf{L}$ and $\mathbf{M}^*$. By calculating the values at the perihelion (closest approach) or the aphelion (farthest approach), we can see that the vector $\mathbf{M}$ points to the perihelion. The magnitude of $\mathbf{M}$ is [see Eq. (3)]

$$|\mathbf{M}|=k\sqrt{1+\frac{2HL^2}{mk^2}}=k\sqrt{1-\frac{L^2}{kma}}, \tag{12}$$

because the energy of a Kepler ellipse is $-k/(2a)$, where a is the semimajor axis. The denominator kma is the square of the maximal angular momentum for an orbit of semimajor axis a, because this case is a circular orbit with constant radius $r=a$ and momentum $p=\sqrt{km/a}$. The square root in Eq. (12) is the eccentricity of the ellipse. So the magnitude of $\mathbf{M}$ is k times the eccentricity (and thus the Runge–Lenz vector is the eccentric perihelion vector).

If we rescale $\mathbf{M}$ [using Eq. (10) and $H=-k/(2a)$], we find that

$$|\mathbf{M}^*|=\sqrt{kma}\,\epsilon, \quad |\mathbf{L}|=\sqrt{kma}\sqrt{1-\epsilon^2}, \tag{13}$$

where ϵ is the eccentricity, $\sqrt{1-b^2/a^2}$, and b is the semiminor axis. Thus the magnitudes of the two vectors determine the size and shape of the ellipse. The directions of the vectors determine the orientation: the orbital plane is perpendicular to $\mathbf{L}$ and the perihelion lies along $\mathbf{M}^*$. Thus the five independent components of $\mathbf{L}$ and $\mathbf{M}^*$ [see the discussion after Eq. (3)] determine the ellipse. Any point in the (negative-energy part of the) six-dimensional phase space can be interpreted in terms of five coordinates determining the Kepler ellipse and a coordinate (like t) that determines the position along the ellipse (see Fig. 1).

Thus, the evolution of a Kepler ellipse under the component M_z^*, for example, is determined by the evolution of $\mathbf{L}$ and $\mathbf{M}^*$ under M_z^*. By Eq. (11) this evolution is given by

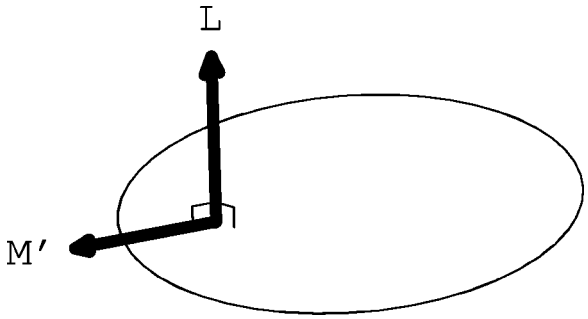

Fig. 1. The angular momentum and Runge–Lenz vectors determine the Kepler ellipse.

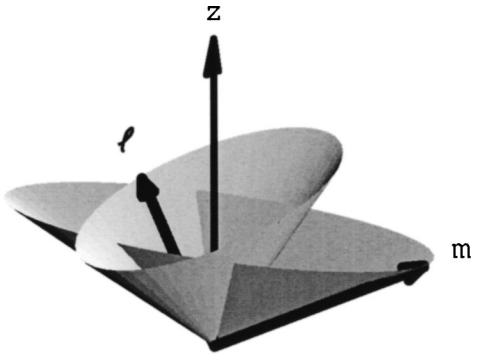

Fig. 2. In the evolution under M_z^*, the scaled angular momentum and Runge–Lenz vectors ℓ and $\mathbf{m}$ trace out elliptical cones about the z-axis.

$$\frac{d\mathbf{L}}{d\lambda}=\{\mathbf{L},M_z^*\}=\hat{\mathbf{z}}\times\mathbf{M}^*, \tag{14a}$$

$$\frac{d\mathbf{M}^*}{d\lambda}=\{\mathbf{M}^*,M_z^*\}=\hat{\mathbf{z}}\times\mathbf{L}. \tag{14b}$$

Note that this evolution maintains $\mathbf{L}\cdot\mathbf{M}^*=0$ and $|\mathbf{L}|^2+|\mathbf{M}^*|^2$ constant. It is convenient to rescale $\mathbf{L}$ and $\mathbf{M}^*$ to make this constant equal to unity by defining

$$\ell=\frac{\mathbf{L}}{\sqrt{kma}},\quad \mathbf{m}=\frac{\mathbf{M}^*}{\sqrt{kma}}, \tag{15}$$

so that

$$\frac{d\ell}{d\lambda}=\hat{\mathbf{z}}\times\mathbf{m},\quad \frac{d\mathbf{m}}{d\lambda}=\hat{\mathbf{z}}\times\ell, \tag{16}$$

with

$$\ell\cdot\mathbf{m}=0,\quad |\ell|^2+|\mathbf{m}|^2=1. \tag{17}$$

[The evolution of ℓ and $\mathbf{m}$ under the original Runge–Lenz generator M_z is the same, just with period $2\pi/\sqrt{-2H/m}$ instead of 2π, as can be seen from Eq. (9) compared to Eq. (11). Entire orbits flow the same under $\mathbf{M}$ and $\mathbf{M}^*$, although individual points do not.]

The system of differential equations (16) is easily solved as

$$\begin{aligned}
\ell_x(\lambda)&=\ell_x(0)\cos\lambda-m_y(0)\sin\lambda,\\
m_x(\lambda)&=-\ell_y(0)\sin\lambda+m_x(0)\cos\lambda,\\
\ell_y(\lambda)&=\ell_y(0)\cos\lambda+m_x(0)\sin\lambda,\\
m_y(\lambda)&=\ell_x(0)\sin\lambda+m_y(0)\cos\lambda,\\
\ell_z(\lambda)&=\ell_z(0),\quad m_z(\lambda)=m_z(0).
\end{aligned} \tag{18}$$

The motion of both ℓ and $\mathbf{m}$ are ellipses in planes of a constant z-component. Some algebra reveals that these two ellipses are identical, except for being rotated by 90° from each other. The major and minor semiaxes of each ellipse in the constant z-component planes are given by

$$r_\pm^2=\frac{1}{2}\big[(1-\ell_z^2-m_z^2)\pm\sqrt{[1-(\ell_z-m_z)^2][1-(\ell_z+m_z)^2]}\big]. \tag{19}$$

The orientation of these ellipses depends on the initial values of the x- and y-components of ℓ and $\mathbf{m}$.

The two vectors thus move along elliptical cones (see Fig. 2), changing their lengths and directions, while staying perpendicular to each other and keeping the sum of the squares of their lengths equal to one. (These elliptical cones can be contrasted with the circular cones along which the two vectors move in the pure rotation generated by components of the angular momentum.) For any pair (ℓ,$\mathbf{m}$), the corresponding Kepler ellipse is perpendicular to the direction of ℓ, has the perihelion along the direction of $\mathbf{m}$, and has eccentricity equal to $|\mathbf{m}|$. Hence, we can see how the ellipse flows under the symmetry transformation generated by M_z^*.

Particularly easy to visualize are the cases in which the elliptical trajectories of ℓ and $\mathbf{m}$ degenerate to lines. From Eq. (19) this occurs in one of two cases: (1) For $\ell_z=0$, the generating component of the Runge–Lenz vector is perpendicular to the angular momentum of the orbit, and thus is in the plane of the orbit. These are the symmetries of the two-dimensional Kepler problem and are discussed in Sec. IV. (2) For $m_z=0$, the generating component of the Runge–Lenz is perpendicular to the orbit's Runge–Lenz vector, as we discuss below. In both cases, we adopt a simplification to display the families of ellipses, that is, we draw the ellipses centered on the origin and make the families easier to visualize. It is trivial to shift the ellipses back to where a focus is at the origin.

For case (2) the initial orbit's major axis is in the x-y plane and we wish to find the family of ellipses generated by flow under M_z^*. As a special case, suppose that the initial orbit is in the x-y plane. In this case the generator is perpendicular to the initial orbital plane. Hence, we take

$$\begin{aligned}
&\ell_x(0)=\ell_y(0)=m_y(0)=m_z(0)=0,\\
&\ell_z(0)=\sqrt{1-m_0^2},\quad m_x(0)=m_0,
\end{aligned} \tag{20}$$

where m_0 is the initial eccentricity. The evolution under M_z^* is

$$\begin{aligned}
&\ell_x(\lambda)=0,\quad \ell_y(\lambda)=m_0\sin\lambda,\quad \ell_z(\lambda)=\sqrt{1-m_0^2},\\
&m_x(\lambda)=m_0\cos\lambda,\quad m_y(\lambda)=0,\quad m_z(\lambda)=0.
\end{aligned} \tag{21}$$

Thus the ellipses all have major axes along x, with the plane of the orbit rotating about x. As the orbits rotate away from the x-y plane, the ellipses become less eccentric until the orbit is circular at $\lambda=\pi/2$. Then the plane rotates back toward x-y, with the ellipses becoming more eccentric. At $\lambda=\pi$, the orbit has the original shape and orientation, but

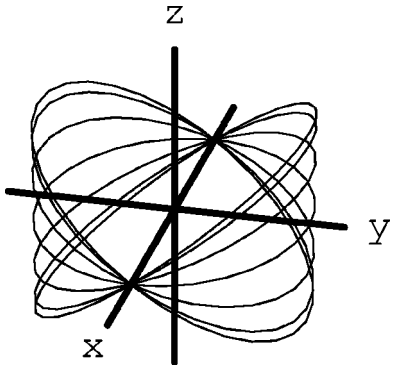

Fig. 3. An ellipse in the x-y plane (major axis along x) under the evolution of M_z^*, drawing the ellipses centered at the origin. (Seven ellipses in the family are shown.) To an observer looking along z at the projection onto the x-y plane, each ellipse in this family looks identical. When the ellipses are drawn properly with the focus at the origin, this observer sees the ellipse simply move sinusoidally in x.

with the other focus at the origin, $\mathbf{m}(\pi)=-\mathbf{m}(0)$. The ellipse undergoes a similar evolution and rotates to the other side of the x-y plane in the second half of the cycle in λ.

The rotation of the ellipse and its change of eccentricity are correlated such that an observer from above, looking at the projection onto the x-y plane, sees no change as the ellipse evolves (assuming that we draw the ellipses centered at the origin). To see this, note that the semimajor axis stays constant, which we can take as $a(\lambda)=1$ (rescaling later if desired). Then the semiminor axis is

$$b(\lambda)=\sqrt{1-\epsilon^2}=\sqrt{1-|\mathbf{m}(\lambda)|^2}=\sqrt{1-m_0^2\cos^2\lambda}. \tag{22}$$

After an evolution for "time" λ, the orbital plane has rotated about x by angle $\psi=\arctan[\ell_y(\lambda)/\ell_z(\lambda)]$. The projection onto the x-y plane shortens the semiminor axis by the factor

$$\cos\psi=\frac{\ell_z(\lambda)}{\sqrt{\ell_y^2(\lambda)+\ell_z^2(\lambda)}}=\frac{\sqrt{1-m_0^2}}{\sqrt{1-m_0^2\cos^2\lambda}}. \tag{23}$$

Thus the projected value of the semiminor axis is

$$b_{\text{proj}}(\lambda)=b(\lambda)\cos\psi=\sqrt{1-m_0^2}, \tag{24}$$

independent of λ (see Fig. 3). [In reality each ellipse has its focus at the origin. The position of the center of the ellipse with respect to the focus is $-a\mathbf{m}(\lambda)=-\hat{\mathbf{x}}a\cos\lambda$ in the x direction. So the projection onto the x-y plane oscillates sinusoidally along the major axis.]

Now return to the general case (2): the initial orbit's Runge–Lenz vector is perpendicular to the generating component M_z^*, but its angular momentum is not necessarily parallel to the generator. We again take the major axis along x so that the initial ellipse is

$$m_x(\lambda)=m_0, \quad \ell_y(0)=\ell_{y0}, \quad \ell_z(0)=\ell_{z0}, \tag{25}$$

with all others zero. From Eq. (18) the evolution under M_z^* is given by

$$m_x(\lambda)=-\ell_{y0}\sin\lambda+m_0\cos\lambda, \tag{26a}$$

$$\ell_y(\lambda)=\ell_{y0}\cos\lambda+m_0\sin\lambda, \tag{26b}$$

$$\ell_z(\lambda)=\ell_{z0}, \tag{26c}$$

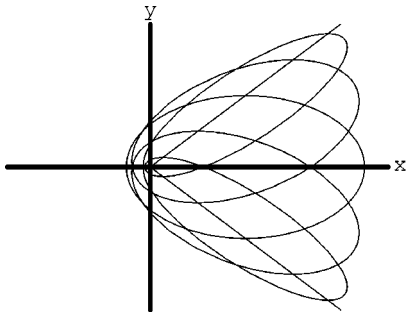

Fig. 4. The evolution of an ellipse in the x-y plane under M_x^*. (Seven ellipses in the family are shown.)

with all others zero. This solution is seen as the same solution (21) as the special case of initial orbit in the x-y plane, but with a different origin for λ. Hence, the family is the same as in Fig. 3, but with the original ellipse not the one in the x-y plane.

IV. TWO-DIMENSIONAL KEPLER PROBLEM

In the other simple special case the generating component M_k^* is in the plane of the initial orbit. Call the plane of the orbit the x-y plane and consider the generator to be a component of $\mathbf{M}^*$ in this plane. The reason for the change in notation is that the evolution of the ellipse remains in the x-y plane. So evolution under Runge–Lenz components in the orbital plane are symmetry operations of the two-dimensional Kepler problem. To show that the evolution stays in the plane, consider the initial ellipse:

$$\begin{aligned}&\ell_x(0)=0, \quad m_x(0)=m_{x0},\\ &\ell_y(0)=0, \quad m_y(0)=m_{y0},\\ &\ell_z(0)=\ell_0, \quad m_z(0)=0,\end{aligned} \tag{27}$$

with $\ell_0=\sqrt{1-m_{x0}^2-m_{y0}^2}$. Then evolution under M_x^* yields

$$\begin{aligned}&m_x(\lambda)=m_{x0}, \quad m_y(\lambda)=m_{y0}\cos\lambda-\ell_0\sin\lambda,\\ &\ell_z(\lambda)=m_{y0}\sin\lambda+\ell_0\cos\lambda,\end{aligned} \tag{28}$$

with all other components zero. For notational simplicity, change the origin of λ to the collision orbit [$\ell(0)=0$, for which the two bodies collide] (see Figs. 4 and 5):

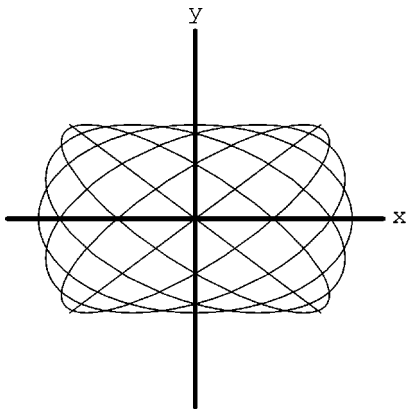

Fig. 5. The same family as Fig. 4, but with the ellipses drawn centered at the origin.

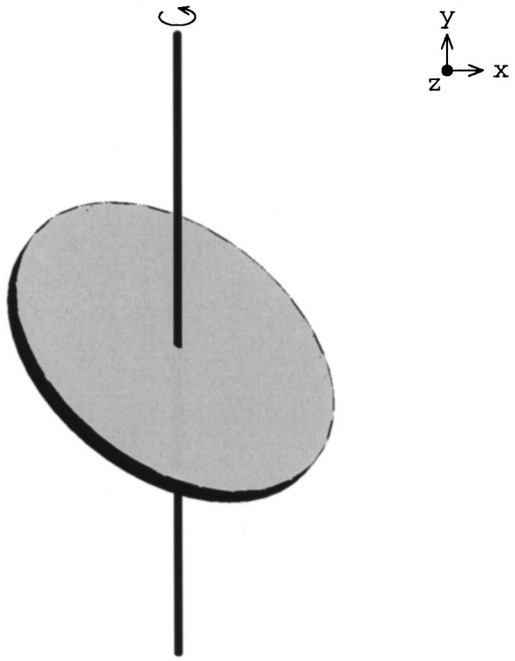

Fig. 6. The family of Fig. 5 is the same as the projection along the z-axis of a certain circle rotated about the y-axis.

$$m_x(\lambda)=\sqrt{1-m_{y0}^2},\quad m_y(\lambda)=m_{y0}\cos\lambda,$$
$$\ell_z(\lambda)=m_{y0}\sin\lambda. \tag{29}$$

The evolution of this ellipse in the x-y plane (drawn centered at the origin) is exactly the same as the projection onto the x-y plane of a rotation of a certain circle in three dimensions. The rotation is about the y-axis and the normal to the circle makes an angle $\theta=\arcsin(m_{y0})$ with that axis. To demonstrate this, note that the normal to the circle after rotation by angle λ about the y-axis is

$$\hat{\mathbf{n}}=(-\sin\theta\cos\lambda,\cos\theta,\sin\theta\sin\lambda). \tag{30}$$

What is the projection onto the x-y plane of this circle with normal $\hat{\mathbf{n}}$? This circle can be rotated into the x-y plane by the angle

$$\chi=\arccos(\hat{\mathbf{z}}\cdot\hat{\mathbf{n}}(\lambda))=\arccos(\sin\theta\sin\lambda), \tag{31}$$

about an axis in the direction $\hat{\mathbf{n}}_{\rm proj}\propto(\cos\theta,\sin\theta\cos\lambda,0)$. Thus the projection of this circle on the x-y plane is an ellipse with a semiminor axis of length,

$$b_{\rm proj}(\lambda)=\cos\chi=\sin\theta\sin\lambda=m_{y0}\sin\lambda, \tag{32}$$

and its major axis in the direction of this rotation axis is

$$\hat{\mathbf{n}}_{\rm proj}\propto(\cos\theta,\sin\theta\cos\lambda,0)=(\sqrt{1-m_{y0}^2},m_{y0}\cos\lambda,0). \tag{33}$$

This sequence of projections is exactly the family (29) of ellipses in two dimensions generated by evolution under M_x^*. This family has the semiminor axis

$$b(\lambda)=\sqrt{1-\epsilon^2(\lambda)}=\sqrt{1-|\mathbf{m}(\lambda)|^2}=m_{y0}\sin\lambda, \tag{34}$$

and a major axis in the direction $(m_x(\lambda),m_y(\lambda))=(\sqrt{1-m_{y0}^2},m_{y0}\cos\lambda)$ (see Fig. 6).

V. GREAT CIRCLES ON SPHERES

That the Kepler ellipses in two dimensions can be thought of as circles in three dimensions seems natural. The symmetry group for the two-dimensional Kepler problem is $O(3)$ (with generators M_x^*, M_y^*, and L_z). This group acts on the unit sphere S^2 of directions in three dimensions, and also on the great circles on the sphere. The line-of-sight projection onto two dimensions presented in Sec. IV is a very simple mapping between the two spaces. However, to make this mapping work, we shifted the ellipses to be centered at the origin. To shift them back to their foci at the origin, the required mapping is more complicated than a Cartesian projection.

Much of the understanding of the symmetry of the Kepler problem has come from mappings to spheres (the three-sphere S^3 in four dimensions for the three-dimensional Kepler problem), although these mappings are different projections onto different spaces than ours. In 1935 Fock[6] showed that the degeneracy of the energy levels of hydrogen could be understood by the symmetry group $O(4)$. He performed a stereographic projection from S^3 onto momentum space,

$$\mathbf{P}=\frac{2\sqrt{-2mE}}{p^2-2mE}\mathbf{p},\quad P_4=\frac{p^2+2mE}{p^2-2mE}. \tag{35}$$

[The sphere is $P_1^2+P_2^2+P_3^2+P_4^2=1$. The South Pole (0,0,0,1) maps to $\mathbf{p}=0$ and the North Pole maps to infinity.] In 1970 Moser[7] constructed a corresponding classical mapping and showed that the Kepler motion is geodesic (free) on the sphere. Thus on that sphere which maps stereographically onto momentum space, the orbits are great circles. Ligon and Schaaf[8] generalized the mapping to make it both canonical and have the simple form for the symmetry generators. Cushman and Duistermaat[9] showed that this mapping is essentially unique and is

$$Q_\alpha=(\mathbf{Q},Q_4)=\frac{1}{k}[A_\alpha(\mathbf{r},\mathbf{p})\sin\phi(\mathbf{r},\mathbf{p})+B_\alpha(\mathbf{r},\mathbf{p})\cos\phi(\mathbf{r},\mathbf{p})], \tag{36a}$$

$$P_\alpha=(\mathbf{P},P_4)=\frac{1}{\sqrt{-2H(\mathbf{r},\mathbf{p})/m}}[-A_\alpha(\mathbf{r},\mathbf{p})\cos\phi(\mathbf{r},\mathbf{p})+B_\alpha(\mathbf{r},\mathbf{p})\sin\phi(\mathbf{r},\mathbf{p})], \tag{36b}$$

where

$$(\mathbf{A},A_4)=\left(k\frac{\mathbf{r}}{r}-(\mathbf{r}\cdot\mathbf{p})\mathbf{p}/m,\sqrt{-2H(\mathbf{r},\mathbf{p})/m}\,\mathbf{r}\cdot\mathbf{p}\right), \tag{37a}$$

$$(\mathbf{B},B_4)=(\sqrt{-2H(\mathbf{r},\mathbf{p})/m}\,r\mathbf{p},rp^2/m-k), \tag{37b}$$

$$\phi(\mathbf{r},\mathbf{p})=\sqrt{-2H(\mathbf{r},\mathbf{p})/m}\,(\mathbf{r}\cdot\mathbf{p}). \tag{37c}$$

[Setting $\phi(\mathbf{r},\mathbf{p})$ to zero essentially gives Fock's and Moser's transformations.]

In these coordinates the symmetry generators are simply

$$L_i=\epsilon_{ijk}Q_jP_k,\quad M_i^*=Q_4P_i-Q_iP_4. \tag{38}$$

The fact that the orbits generated by M_k^* are closed is made obvious in this formulation. M_3^* conserves Q_1, Q_2, P_1, and P_2, in addition to four functions that are immediate from the group commutation relations, M_3^*, L_3, $M_1^{*2}+L_2^2$, and

$M_2^{*2}+L_1^2$. Five of these eight relations are independent, leaving a one-dimensional space left for the trajectory. However, it appears from the form of these functions that this trajectory cannot be written down in closed form.

ACKNOWLEDGMENT

I thank Matthias Reinsch for many useful discussions.

[a]Electronic mail: email_jim_morehead@yahoo.com

[1]H. Goldstein, *Classical Mechanics* (Addison-Wesley, 1980), 2nd ed., Sec. 3.9.
[2]Several months before Schrödinger published his famous equation, Pauli used these commutation relations and Heisenberg's matrix mechanics to find the spectrum of hydrogen, including explaining the ''accidental'' degeneracy due to the extra symmetry (Refs. 3–5).
[3]W. Pauli, ''Über das Wasserstoffspektrum vom Standpunkt der neuen Quantenmechanik,'' Z. Phys. **36**, 336–363 (1926).
[4]G. Baym, *Lectures on Quantum Mechanics* (W. A. Benjamin, Reading, Massachusetts, 1973), pp. 175–178.
[5]A. Bohm, *Quantum Mechanics: Foundations and Applications* (Springer-Verlag, Berlin, 1979), Chap. VI.
[6]V. Fock, ''Zur Theorie des Wasserstoffatoms,'' Z. Phys. **98**, 145–154 (1935).
[7]J. Moser, ''Regularization of Kepler's problem and the averaging method on a manifold,'' Commun. Pure Appl. Math. **23**, 609–636 (1970).
[8]T. Ligon and M. Schaaf, ''On the global symmetry of the classical Kepler problem,'' Rep. Math. Phys. **9**, 281–300 (1976).
[9]R. H. Cushman and J. J. Duistermaat, ''A characterization of the Ligon-Schaaf regularization map,'' Commun. Pure Appl. Math. **50**, 773–787 (1997).

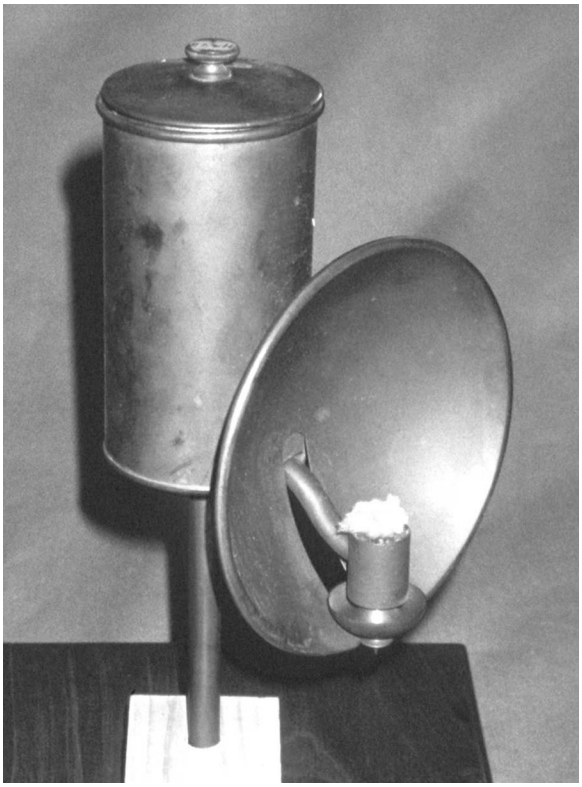

Locatelli's Lamp. Locatelli's lamp was used as a source for experiments on thermal radiation. The lamp burns alcohol in the wick placed at the focal point of the polished copper reflector. There is no chimney, and the cylindrical tank holds the alcohol. This lamp, from the Greenslade Collection, was sold by Max Kohl of Chemnitz for 14.50 marks at around 1900. It is shown in the Kohl catalogue as part of a complete set of apparatus that was mounted on an optical bench. (Photograph and notes by Thomas B. Greenslade, Jr., Kenyon College)